ISSN 0029-3865

CBPF - CENTRO BRASILEIRO DE PESQUISAS FÍSICAS

Rio de Janeiro

Notas de Física

CBPF-NF-011/12
May 2012

Simple description of cluster radioactivity

O A P Tavares and E L Medeiros

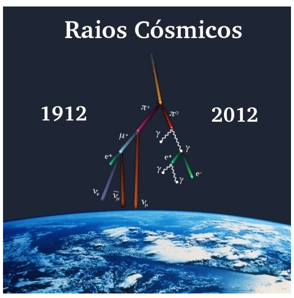

50 anos
PÓS-GRADUAÇÃO CBPF

Ministério da
Ciência, Tecnologia
e Inovação

CBPF-NF-011/12

Simple description of cluster radioactivity[1]

O A P Tavares and E L Medeiros[2]

Centro Brasileiro de Pesquisas Físicas - CBPF/MCTI

Rua Dr. Xavier Sigaud 150, 22290-180 Rio de Janeiro-RJ, Brazil

Abstract - The partial half-life of radioactive decay of nuclei by the emission of fragments heavier than the alpha particle, such as the emission of carbon, oxygen, neon, magnesium, and silicon isotopes from translead nuclei (known as cluster radioactivity), is re-evaluated in the framework of a semiempirical, one-parameter model based on the quantum mechanical tunneling mechanism through a potential barrier where the Coulomb, centrifugal, and overlapping contributions to the barrier are considered within the spherical nucleus approximation. This treatment has shown not only very adequate to fit all the existing half-life data, but also to give more reliable half-life predictions for new, yet unmeasured cases of spontaneous emission of massive nuclear fragments both from heavy and intermediate-mass parent nuclei as well.

PACS number: 23.70.+j

[1]In celebration of the eightieth anniversary of the discovery of the neutron.

[2]Corresponding author. E-mail: emil@cbpf.br

1 Introduction

The process of spontaneous emission of nuclear fragments heavier than the alpha particle, known as cluster (or exotic) radioactivity, observed in the translead nuclei has been described by several authors, and it is a nuclear process firmly established nowadays (see, for instance, Refs. [1–17] and references quoted therein). Since the detection for the first time in 1983 of ^{14}C ions emitted from a source of ^{223}Ra isotope by Rose and Jones from the University of Oxford [18], and promptly confirmed independently by several research groups [19–22], a number of cases for cluster radioactivity of heavy nuclei (from ^{221}Fr up to ^{242}Cm) have been observed which involve the emission of fragments even heavier than ^{14}C such as ^{20}O, ^{23}F, $^{22,24-26}$Ne, ^{28,30}Mg, and ^{32,34}Si isotopes [6, 12]. The latest case observed to date has been the emission of ^{14}C from ^{223}Ac parent nucleus, as reported by Guglielmetti *et al.* [23]. It appears that cluster radioactivity is indeed a very rare nuclear process since the observed branching ratio relative to alpha decay varies from 5×10^{-17} (^{238}Pu $\rightarrow$ ^{32}Si) to 4.1×10^{-9} (^{223}Ra $\rightarrow$ ^{14}C).

The possible existence for such a rare spontaneous disintegration process was considered quantitatively for the first time early in 1975–1976 by de Carvalho *et al.* [24, 25], when very preliminary calculations based on the classical WKB method for penetration through a potential barrier indicated the possibility of a few heavy fragments in the mass range 20–70 being emitted from ^{238}U. These calculations were motivated by the observation of short-range tracks (as compared to ordinary fission fragment tracks) recorded in nuclear-track emulsion that had been loaded with a solution of natural uranium aimed at remeasuring its spontaneous-fission half-life. At that time it was supposed that those shorter-range tracks had originated from a case of emission of large nucleon clusters of intermediate-mass in the region from neon to nickel [26, 27]. Those early calculations showed that shell effects were clearly manifested since results had indicated the processes involving magic numbers either for the emitted fragment or daughter product (or both) as the most likely emission modes (a historical account on this subject is briefly reported in [11, 28]).

These surprising, novel results were interpreted soon after by Săndulescu and Greiner [29, 30] as a case of very large asymmetry in the break-up of heavy fissile nuclei caused by shell effects of one or both fragments. Later on, more refined and improved calculations showed that the new radioactive process could be interpreted either as a highly mass-asymmetric fission mode or as an emission of intermediate-mass nucleon clusters between the alpha particle and ordinary fission fragments [31–33]. These theoretical investigations on exotic decays have stimulated a number of experimental research groups to identify and measure the activity in rare possible cases of cluster radioactivity of extremely small ($\sim 10^{-16}$–10^{-9}) predicted branching ratio relative to alpha decay. Today, twenty-seven cases of exotic decays have been experimentally identified in the region of translead parent nuclei. Detailed descriptions for this phenomenon from both the experimental and theoretical points of view can be found in Refs. [4–7, 9, 10, 15–17, 34–36], and, quite recently, descriptions of heavy-particle radioactivity are being considered for superheavy nuclei [37, 38] as well as new unified treatments to cluster and alpha radioactivities became available [13, 14].

In a recent past we were successful in developing a one-parameter model to systematize the alpha decay half-life data of bismuth isotopes [39], and, afterwards, this routine calculation showed again very adequate to systematize the half-lives of cases for alpha decay of platinum isotopes [40, 41], heavy-cluster radioactivity of translead nuclei [11] as well as radioactivity by proton emission observed in very neutron-deficient complex nuclei [42, 43]. In the present paper we thought it worthwhile to apply our original model description [39], but introducing a slight modification concerning the dependence of the one-parameter of the model with cluster radius to obtain a unique, universal trend for the half-life of all cases of cluster decay. The present description can be useful to obtain half-life evaluations for new cases of exotic decays not yet experimentally observed and for heavy-fragment emission modes of heavy and intermediate-mass parent nuclei as well.

2 Semiempirical treatment to cluster radioactivity

The one-parameter model to half-life evaluation of heavy-fragment decay cases has been reported in details in our previous papers [11, 39, 41], and it is based on the current, quantum mechanical tunneling mechanism through a Coulomb-plus-centrifugal-plus-overlapping potential barrier constructed within the spherical nucleus approximation. In brief, the decay constant, λ, is given by the product of three quantities, namely,

$$\lambda = \lambda_0 SP, \quad S = \mathrm{e}^{-G_{\mathrm{ov}}}, \quad P = \mathrm{e}^{-G_{\mathrm{se}}}, \tag{1}$$

in which λ_0 represents the number of assaults on the barrier per unit time, S is the cluster preformation probability at the nuclear surface, and P is the penetrability factor through the external, separation barrier region, *i.e.* the Coulomb-plus-centrifugal potential barrier. The frequency factor λ_0 has been evaluated as

$$\lambda_0 = \frac{v}{2a} = \frac{\sqrt{2}}{2a}\sqrt{\frac{Q}{\mu_0}}\,, \tag{2}$$

where v is the relative velocity of the fragments, $a = R_{\mathsf{P}} - R_{\mathsf{C}}$ is the difference between the radius of the parent nucleus and the cluster radius, μ_0 is the final reduced mass of the system (see below), and Q is the total disintegration energy, *i.e.* the Q-value for the decay process. In (1), the G's are the classical WKB-integral approximation (Gamow's factor for decay) given by

$$G = \frac{2}{\hbar}\int_{s_1}^{s_2}\sqrt{2\mu(s)\left[V(s) - Q\right]}\,\mathrm{d}s \tag{3}$$

where s is the separation between the centres of the fragments (the emitted cluster and daughter, residual nucleus), $V(s)$ is the potential barrier, and $\mu(s)$ is the reduced mass of the disintegration system.

Gamow's factor G_{ov} is calculated in the overlapping barrier region where the cluster to be emitted drives away from the parent nucleus ($s_1 = a = R_{\mathsf{P}} - R_{\mathsf{C}}$) until the configuration at contact of the preformed fragments is reached ($s_2 = c = R_{\mathsf{D}} + R_{\mathsf{C}}$; here, R_{D} denotes the radius of the daughter nucleus). The quantity $S = \mathrm{e}^{-G_{\mathsf{ov}}}$ represents, therefore, the preformation probability, or the "arrival" of the cluster to the nuclear surface. S is sometimes known as the spectroscopic factor, which is strongly related to the complexity of the cluster to be preformed.

On the other hand, G_{se} is calculated through the external, separation barrier region which extends from $s_1 = c$ up to the separation point $s_2 = b$ where the total potential energy equals the Q-value for decay, *i.e.* $V(b) = Q$.

In the overlapping region, following previous descriptions by Duarte and Gonçalves [44] and Poenaru *et al.* [1] to $\mu(s)$ and $V(s)$, respectively, both these quantities have been assumed to follow power functions of s ($a \leq s \leq c$) such that

$$\mu(s) = \mu_0\left(\frac{s-a}{c-a}\right)^p\,, \quad p \geq 0\,, \tag{4}$$

$$V(s) = Q + (V_{\mathsf{c}} - Q)\left(\frac{s-a}{c-a}\right)^q , \quad q \geq 1 , \tag{5}$$

where the total potential energy at contact configuration, V_{c} , is given by

$$V_{\mathsf{c}} = \frac{Z_{\mathsf{C}} Z_{\mathsf{D}} e^2}{c} + \frac{\ell(\ell+1)\hbar^2}{2\mu_0 c^2} , \tag{6}$$

in which $e^2 = 1.4399652$ MeV·fm is the square of the electronic elementary charge, ℓ is the mutual orbital angular momentum resulting from the rotation of the disintegration product nuclei around their common centre of mass, $\hbar = h/2\pi$ is Planck's constant, and the Z's are the atomic numbers.

In the separation region ($c \leq s \leq b$) the effective reduced mass of the already defined fragments is constant, μ_0, given by $\mu_0^{-1} = m_{\mathsf{C}}^{-1} + m_{\mathsf{D}}^{-1}$, and the potential energy is calculated as the ordinary $1/s$-Coulomb plus $1/s^2$-centrifugal potentials. Here, the m's denote nuclear (rather than atomic) mass-values (see below). Figure 1 shows the potential barrier $V(s)$ for three cases of cluster radioactivity ($\ell = 0$) where the overlapping and separation regions are clearly evidenced, as well as the differences in the shape of the potential between each other case.

Accordingly, from the above considerations and assumptions, and by expressing lengths in fm, masses in u, energies in MeV, and time in s, the half-life has been computed as

$$\tau = \log_{10} T_{1/2} = \log_{10}\left[\frac{\ln 2}{\lambda}\right] = \tau_0 + \tau_1 + \tau_2 , \tag{7}$$

where

$$\tau_0 = -22 + \log_{10}\left[a\,(\mu_0/Q)^{1/2}\right] \tag{8}$$

is the term related to the frequency of assaults on the barrier,

$$\tau_1 = 0.19\,(c-a)\,g\,\sqrt{\mu_0 Q}\,H(x,y) \tag{9}$$

is the contribution from the overlapping barrier region, and

$$\tau_2 = 0.27358\,Z_{\mathsf{D}} Z_{\mathsf{C}}\,(\mu_0/Q)^{1/2}\,F(x,y) \tag{10}$$

is the one corresponding to the external, separation barrier region. The functions $H(x,y)$ and $F(x,y)$ contain the dependence upon angular momentum, ℓ, and they are given by

$$H(x,y) = (x + 2y - 1)^{1/2} , \tag{11}$$

$$F(x,y) = \frac{x^{1/2}}{2y} \cdot \ln \frac{x^{1/2} H(x,y) + x + y}{\sqrt{x+y^2}} + \arccos \left[\frac{1}{2} \left(1 - \frac{y-1}{\sqrt{x+y^2}} \right) \right]^{1/2} - \frac{H(x,y)}{2y} \,, \quad (12)$$

where the quantities x and y are defined as

$$x = \frac{20.9008\, \ell(\ell+1)}{\mu_0 c^2\, Q} \,, \qquad y = \frac{1}{2} \frac{Z_{\mathsf{C}} Z_{\mathsf{D}} e^2}{c\, Q} \,. \quad (13)$$

Expressions (11) and (12) are valid for all values of $x \geq 0$ and $y > 1/2$. In the present description, g (which appears in equation (9)) is the only adjustable parameter, the value of which being thus determined from a set of half-life measurements (see below). In solving the G_{ov} WKB-integral (eqs. (3)–(6)), parameter g results as a combination of the unknown exponents p and q, namely,

$$g = \left(1 + \frac{p+q}{2} \right)^{-1} \,, \qquad 0 < g \leq 2/3 \,. \quad (14)$$

The semiempirical g-value depends upon the source data for both nuclear mass and radius as well as the set of measured half-lives for the different cluster emission cases. The g-value is related through eq. (9) to the strength of the spectroscopic factor, *i.e.*, the cluster preformation probability.

Finally, for the particular cases of $\ell = 0$ it results $x = 0$, and the expressions (9) and (10) are transformed, therefore, to

$$\tau_1 = 0.19\, (c-a)\, g\, \sqrt{\mu_0 Q}\, \sqrt{u^{-1} - 1} \,, \quad (15)$$

and

$$\tau_2 = 0.27358\, Z_{\mathsf{C}} Z_{\mathsf{D}}\ (\mu_0/Q)^{1/2}\, F(u) \,, \quad (16)$$

in which

$$F(u) = \arccos \sqrt{u} - \sqrt{u(1-u)} \,, \quad u = (2y)^{-1} \,. \quad (17)$$

3 Basic quantities and input data

To apply the present routine calculation to half-life evaluations of nuclear decay cases by cluster emission, the source for three basic quantities should be specified. These quantities are: *i*) nuclear mass, *ii*) nuclear radius, and *iii*) angular momentum associated to the ground-state to ground-state transitions. The values for both the quantities Q and μ_0 have been evaluated from the nuclear (rather than atomic) mass-values of the participating nuclides, namely,

$$Q = m_{\mathsf{P}} - (m_{\mathsf{D}} + m_{\mathsf{C}})\,, \quad \mu_0^{-1} = m_{\mathsf{D}}^{-1} + m_{\mathsf{C}}^{-1}\,, \tag{18}$$

where the m's are given by

$$m_i = A_i - Z_i m_{\mathsf{e}} + \left(\Delta M_i + k Z_i^{\beta}\right)/F\,, \quad i = \mathsf{P}, \mathsf{D}, \mathsf{C}\,, \tag{19}$$

in which $F = 931.494009$ MeV/u is the mass-energy conversion factor, $m_{\mathsf{e}} = 0.54858 \times 10^{-3}$ u is the electron rest mass, and ΔM is the atomic mass-excess evaluation as tabulated by Audi *et al.* [45] (the 2003 AME or AME03). The quantity kZ^{β} represents the total binding energy of the Z electrons in the atom, where the values $k_1 = 8.7 \times 10^{-6}$ MeV and $\beta_1 = 2.517$ for nuclei of $Z \geq 60$, and $k_2 = 13.6 \times 10^{-6}$ MeV and $\beta_2 = 2.408$ for $Z < 60$ have been found from data reported by Huang *et al.* [46]. In this way, the Q-value for decay is calculated as

$$Q = \Delta M_{\mathsf{P}} - (\Delta M_{\mathsf{D}} + \Delta M_{\mathsf{C}}) + \left[k_1 \left(Z_{\mathsf{P}}^{\beta_1} - Z_{\mathsf{D}}^{\beta_1}\right) - k_2 Z_{\mathsf{C}}^{\beta_2}\right]\,, \tag{20}$$

where the term in brackets represents the effect of the screening to the nucleus caused by the surrounding electrons.

The spherical nucleus approximation has been adopted to the present calculation model, and the nuclear radius-values, R_i ($i = \mathsf{P}, \mathsf{D}, \mathsf{C}$), have been evaluated following the droplet model of atomic nuclei [47, 48]. Accordingly, the following radius expressions for the average equivalent root-mean-squares radius of the proton and neutron density distributions have been used throughout:

$$R_i = \frac{Z_i}{A_i} R_{\mathsf{p}i} + \left(1 - \frac{Z_i}{A_i}\right) R_{\mathsf{n}i}\,, \quad i = \mathsf{P}, \mathsf{D}, \mathsf{C}\,. \tag{21}$$

Here the equivalent proton and neutron radii R_{ji} are given by

$$R_{ji} = r_{ji} \left[1 + \frac{5}{2}\left(\frac{w}{r_{ji}}\right)^2\right]\,, \quad j = \mathsf{p}, \mathsf{n}\,, \tag{22}$$

in which $w = 1$ fm is the diffuseness of the nuclear surface, and the $r_{ji}{}'$s denote the equivalent sharp radius of the proton ($j = \mathsf{p}$) or neutron ($j = \mathsf{n}$) density distributions. These latter quantities, in turn, are calculated following the finite-range droplet model description of nuclei by Möller *et al.* [48], being given by

$$r_{\mathsf{p}i} = r_0\left(1+\overline{\epsilon_i}\right)\left[1-\frac{2}{3}\left(1-\frac{Z_i}{A_i}\right)\left(1-\frac{2Z_i}{A_i}-\overline{\delta_i}\right)\right]A_i^{1/3}, \qquad (23)$$

$$r_{\mathsf{n}i} = r_0\left(1+\overline{\epsilon_i}\right)\left[1+\frac{2}{3}\frac{Z_i}{A_i}\left(1-\frac{2Z_i}{A_i}-\overline{\delta_i}\right)\right]A_i^{1/3}, \qquad (24)$$

where

$$\overline{\epsilon_i} = \frac{1}{4\,\mathrm{e}^{0.831A_i^{1/3}}} - \frac{0.191}{A_i^{1/3}} + \frac{0.0031Z_i^2}{A_i^{4/3}}, \qquad (25)$$

$$\overline{\delta_i} = \left(1-\frac{2Z_i}{A_i}+0.004781\frac{Z_i}{A_i^{2/3}}\right)\Bigg/\left(1+\frac{2.52114}{A_i^{1/3}}\right), \qquad (26)$$

and $r_0 = 1.16$ fm. Although this radius parametrization is valid for nuclei from ^{16}O on, we decided to extend it down to ^{14}C without any detriment of the systematic analysis of the data. Figure 2 shows the reduced radius, $R/A^{1/3}$, of the equivalent liquid-drop model of the nucleus plotted against mass number. The trend reveals a strong decrease of reduced radius when one passes from less-massive nuclei to heavy and superheavy ones, thus reflecting a clear degree of nuclear compressibility.

Finally, the values of mutual angular momentum, ℓ, have been obtained from the usual nuclear spin ($\boldsymbol{J}$) and parity (π) conservation laws ($\boldsymbol{J}_{\mathsf{P}} = \boldsymbol{J}_{\mathsf{D}} + \boldsymbol{J}_{\mathsf{C}} + \boldsymbol{\ell}$, $\pi_{\mathsf{P}} = \pi_{\mathsf{D}} \cdot \pi_{\mathsf{C}}(-1)^{\ell}$), where the values for the different J's and π's (when available) are those reported in [45]. Sometimes, in cluster radioactivity it is not possible to evaluate the ℓ-value (particularly for heavy cluster emission cases) but, fortunately, the influence of the ℓ-values (up to $\ell = 10$ or so) on calculated half-life is not significant in these cases because the value of x is always very small (see eqs. (11)–(13)), and, therefore, $H(x,y) \approx H(0,y)$ and $F(x,y) \approx F(0,y)$, which makes $\tau = \log_{10} T_{1/2}$ practically unchanged.

The input data for all experimentally known cases of exotic radioactivity have been taken from the literature [6, 7, 9, 11, 12, 23], and they reach the total of fifty-nine measured half-life-values for twenty-seven distinct cases of heavy-ion emission from twenty different translead parent nuclei. In about half of the decay cases all nuclei involved in are of the even-even type, therefore $\ell = 0$. In the other cases ℓ can take only one among the values 1, 2, 3, or 4 depending upon nuclear spin and parity values of the participating nuclides. Q-values for different cluster emissions investigated experimentally are in the range $\sim$28 MeV

(^{226}Ra → ^{14}C)–97 MeV (^{242}Cm → ^{34}Si), thus corresponding to a small variation of ∼ 1.9–2.4 MeV/u in the kinetic energy of the emitted cluster. The branching ratio relative to alpha decay of the parent nuclei, $b_\alpha = \lambda_{\mathsf{C}}/\lambda_\alpha$, is of great importance to experimental identification of an emitted heavy-ion. Values of b_α have been found as low as 5×10^{-17} (for the case ^{238}Pu → ^{32}Si) up to 4×10^{-9} (^{223}Ra → ^{14}C).

4 Semiempirical determination of parameter *g*

To proceed with a systematic analysis of the partial half-life for nuclear exotic decays, firstly we applied our routine calculation method to obtain the semiempirical value of the one-parameter, g, of the present model. Two methods have been used, namely: *i*) a best g-value is found out in such a way the standard deviation

$$\sigma = \left[\frac{1}{n-2}\sum_{i=1}^{n}(\tau_i^{\mathsf{c}} - \tau_i^{\mathsf{e}})^2\right]^{1/2} \tag{27}$$

becomes a minimum. Here, the superscripts denote calculated (τ^{c}) or experimental (τ^{e}) values of the decimal logarithm of the half-life, and $n = 59$ is the number of cases considered. This gives a best g-value of $g = 0.349$ corresponding to a $\sigma_{\mathsf{min}} = 0.81$; *ii*) the g-value could alternatively be determined as the average of the individual g-values obtained for each decay case by inverting eq. (7), *i.e.*,

$$g = \frac{\tau^{\mathsf{e}} + 22 - \log\left[a(\mu_0/Q)^{1/2}\right] - 0.27358 Z_{\mathsf{C}} Z_{\mathsf{D}} (\mu_0/Q)^{1/2} F(x,y)}{0.19\,(c-a)\sqrt{\mu_0 Q}\,H(x,y)}\,. \tag{28}$$

In this way, a value $\overline{g} = 0.349 \pm 0.021$ has been found by using all the existing half-life data. Figure 3 shows the individual g-values plotted against mass asymmetry, $\eta = 1 - 2A_{\mathsf{C}}/A_{\mathsf{P}}$ (note that $\eta \lesssim 0.40$ for fission process, $0.40 \lesssim \eta \lesssim 0.92$ for cluster emission, $0.92 \lesssim \eta \lesssim 0.96$ for α-decay, and $\eta \gtrsim 0.96$ for cases of radioactivity by proton emission). It is clear from fig. 3 that a unique g-value should be associated to all cases of cluster radioactivity. Of course, the g-value obtained by either method *i*) or *ii*) above depends upon the choice for the source of data related to nuclear mass (the AME03 [45], FRDM95 [48], or AME11 [50], and others) as well as nuclear radius (different systematics for root-mean-squares radius of the charge or neutron distributions, sharp radius of proton or neutron distributions, equivalent proton or neutron radius, and so on). In our previous study [11], for instance, the radius-values adopted for the emitted clusters, R_{C}, were the average of the rms-radius evaluation of the neutron and proton density distributions following the parametrization by Dobaczewski *et al.* [49], thus giving $R_{\mathsf{C}}/A_{\mathsf{C}}^{1/3}$-values in the range ~ 1.02–1.13 fm, therefore resulting in a value $\overline{g} = 0.260 \pm 0.024$, *i.e.* $\sim 25\%$ lower than that obtained in the present analysis. Another example is the result $\overline{g} = 0.300 \pm 0.026$ which is obtained by choosing the same reduced radius-value $R/A^{1/3} = 1.205$ fm for all parent, daughter, and emitted nuclei. A general rule thus emerges from inspection on eq. (28): an increase in nuclear radius or Q-value (or in both these quantities) leads to an increase in g-value. From the physics point of view, this is because whatever the case the effective potential barrier (of both the overlapping and separation regions) becomes lower, therefore g will result greater to compensate for half-life. The conclusion can be drawn that once a mass-table and/or radius parametrization have been chosen, all subsequent half-life evaluations should be made by using these mass- and radius-values with which the semiempirical g-value has been obtained. Accordingly, option has been made for the AME03 mass-table [45] and the radius parametrization following the FRDM in the spherical approximation [48] to be used throughout the present description.

5 Systematics of half-life for exotic decays

The semiempirical determination of the one-parameter ($\overline{g} = 0.349 \pm 0.021$) of the present calculation model is now inserted back into eq. (9), thus allowing the evaluation of the half-lives and subsequent comparison with the experimental half-life data. In addition, half-life predictions for new, not yet experimentally investigated heavy-ion emission cases can be obtained at the utmost within two orders of magnitude. However, a simple, global description and systematization of the known data can be presented following the methodology developed, for instance, in [41], where the Coulomb (τ_2^{coul}) and centrifugal (τ_2^{cent}) contributions to the external, separation barrier region are completely separated from each other such that, in eq. (10), $\tau_2 = \tau_2^{\mathsf{coul}} + \tau_2^{\mathsf{cent}}$. It suffices to write the "penetrability" function $F(x,y)$ as

$$F(x,y) = F(0,y) + [F(x,y) - F(0,y)] \; , \tag{29}$$

and, after substitution into eq. (10) gives

$$\tau_2^{\mathsf{coul}} = 0.27358z\,, \quad z = Z_{\mathsf{C}} Z_{\mathsf{D}} \left(\mu_0/Q\right)^{1/2} \cdot F(0,y)\,, \tag{30}$$

where, as before, $F(0,y) \equiv F(u)$ (cf. equation (17)). Now, one defines the "reduced" half-life, τ_{r}, by subtracting from the half-life all its contributions other than the Coulomb one, *i.e.*

$$\tau_{\mathsf{r}} = \tau - (\tau_0 + \tau_1 + \tau_2^{\mathsf{cent}}) \equiv \tau_2^{\mathsf{coul}} = 0.27358z\,. \tag{31}$$

This means that $\tau_{\mathsf{r}} \equiv \tau_2^{\mathsf{coul}}$ should be proportional to the Coulomb parameter z as given by (30), and, therefore, τ_{r} does not depend upon angular momentum ℓ. The present methodology has proved quite satisfactory in analysing decay data for radioactivity by proton emission [43] and alpha decay [41] as well.

The same happens to all known cases of exotic decays, as can be appreciated in figure 4. Data points defined by pairs of values $(z, \tau_{\mathsf{r}}^{\mathsf{e}})$ in figure 4 are seen indeed very close to the straight line $\tau_{\mathsf{r}}^{\mathsf{c}} = 0.27358z$ irrespective of ℓ-values (see inset histogram). All data showed in figure 4 fit the straight line within two standard deviations (this corresponds to $\sigma \approx$ 1.60 orders of magnitude). Only in one case (^{236}U $\rightarrow$ ^{30}Mg + ^{206}Hg [51], filled rhomb) the difference $\Delta\tau = \tau^{\mathsf{c}} - \tau^{\mathsf{e}}$ amounts to 1.58, which represents a quite acceptable level of reproducibility. The inset graph shows the relative positions between the actual data for translead parent nuclei ($87 \leq Z_{\mathsf{P}} \leq 96$, full symbols) and exotic decay cases that could eventually occur in the region of superheavy parent nuclei ($Z_{\mathsf{P}} > 103$, open symbols).

6 Cluster radioactivity in the heaviest nuclei

The present routine calculation has been used in this study to estimate partial half-lives of heavy cluster ($Z_{\mathsf{C}} \geq 14$) radioactivity in the region of the heaviest actinide parent nuclei. Exotic decay cases have been selected in such a way that the daughter nucleus is preferably either a neutron-magic, the double magic ^{208}Pb or its nearest nuclei as, for instance, ^{203,204}Pt, ^{204,205}Au, ^{205,206}Hg, $^{206–209}$Tl, $^{206–212}$Pb, and $^{209–213}$Bi isotopes. In addition, the most likely candidates to be considered as a heavy cluster ($Z_{\mathsf{C}} \geq 14$) are those selected according to Ronen's 'golden rule' for exotic decays [52], *i.e.*, those nuclei which have the highest average binding energy per total number of deuterons and tritons. Ronen, besides the aspects related to shell effects, has considered nuclei as composed of blocks of deuterons and tritons. Accordingly, the average binding energy per deuteron-plus-triton is calculated as

$$\overline{B}_{\mathsf{d+t}}(Z,A) = 10.01855 + \frac{1}{Z}\,[1.8140846A - \Delta M] - 1.36\times 10^{-5} Z^{1.408}\ \mathrm{MeV}\,, \qquad (32)$$

where ΔM is the atomic mass excess values (in MeV) taken from [45], and the expression above is restricted to nuclei of $2Z \leq A \leq 3Z$. Following Ronen's rule ^{28}Mg should be, among magnesium isotopes, the most likely candidate to be emitted. Indeed, this is the case since ^{28}Mg has been observed as the emitted cluster from ^{234}U and ^{236,238}Pu parent nuclei producing ^{206}Hg and ^{208,210}Pb as daughter nuclei, respectively (the case ^{236}Pu $\to$ ^{28}Mg + ^{208}Pb is the most likely to occur in view of the strong shell effect due to the double magic ^{208}Pb). Another example is the preference for ^{32}Si isotope (which shows the greatest $\overline{B}_{\mathsf{d+t}}$) as a cluster to be emitted, but ^{34}Si combined with ^{208}Pb in the decay of ^{242}Cm is $\sim$2 orders of magnitude more likely to occur than the case ^{238}Pu $\to$ ^{32}Si + ^{206}Hg (again, the strong influence of the double magic ^{208}Pb daughter nucleus). The same happens when neon isotopes are seen as emitted clusters. In fact, ^{24}Ne and ^{22}Ne, which exhibit the greatest values of $\overline{B}_{\mathsf{d+t}}$ (14.97 and 14.81 MeV, respectively) have been observed in seven (six as ^{24}Ne and one as ^{22}Ne emissions) of the ten cases of exotic decays which produce neon isotopes, the most likely decay cases occurring with formation of ^{208}Pb daughter nucleus.

Figure 5 shows, for a sample of isotopic sequences of clusters, the behavior of $\overline{B}_{\mathsf{d+t}}$ in a comparison with that exhibited by ordinary average binding energy per nucleon, $\overline{B}_{\mathsf{p+n}}$. Except for the double magic ^{16}O the position of the maxima in $\overline{B}_{\mathsf{d+t}}$ does not coincide with the ones of $\overline{B}_{\mathsf{p+n}}$. Therefore, we decided to use the "golden rule" mentioned above as a guide to choose cluster candidates to be emitted and, thus, consider those nuclei located around the maximum of $\overline{B}_{\mathsf{d+t}}$ in each Z_{C}-sequence. Finally, a daughter nucleus and cluster emitted, both selected following Ronen's golden rule, are combined in such a way to form heavy parent nuclei of longest measured total half-life. These latter have been considered in estimating their partial half-life for cluster radioactivity. Table 1 lists a number of exotic radioactivity cases chosen according to the criteria here described. Only cases of emitted clusters with $Z_{\mathsf{C}} \geq 14$, half-lives $\tau = \log T_{1/2}\,(\mathrm{s}) \lesssim 28$, and branching ratio relative to alpha decay $\log b_\alpha \gtrsim -20$ have been displayed. Of special interest and importance are the cases of product nuclei of either 20, 28, and 126 neutron- or 20 and 82 proton-shell closures (or both) and their neighbours. Mass asymmetry of the various processes listed in Table 1 is in the range 0.600–0.740. τ-values obtained following the methodology of the present work (10$^{\text{th}}$ column) show uncertainties within about 1–2 units, *i.e.* 1–2 orders of magnitude in the half-life (see section 7). The present results can be compared to results (when available) reported by Poenaru *et al.* [3] and Duarte *et al.* [8]. These latter ones (12$^{\text{th}}$ column) are systematically lower than both the present estimates and the ones of Ref. [3]. Good agreement (differences not greater than ~ 2 orders of magnitude) is achieved between the present results and those obtained by the ASAFM calculation of Ref. [3]. Table 1 shows, in addition, the most likely cases predicted to occur in heavy cluster radioactivity, namely, the emission of ^{32}Si from ^{236,237}Np, ^{238}Pu and ^{240}Cm isotopes, and ^{34}Si from ^{238}U, ^{239,240}Pu, ^{241}Am, and ^{242,243}Cm parent nuclei for which cases the branching ratio to alpha decay is evaluated as $b_\alpha \gtrsim 10^{-16}$. Harder to be observed are the cases for the emission of ^{32}Si from ^{241}Am and ^{242}Cm parent nuclei, ^{34}Si from ^{243}Am and ^{240}Cm emitter nuclides, as well as ^{48}Ca from ^{252}Es and ^{50}Ca from ^{258}Md. Rather unlikely of being detected are also the emission cases for ^{46}Ar from ^{252}Cf and ^{254}Es, ^{50}Ca from ^{254}Es, and ^{49,50}Ca from ^{259}No parent nuclei. For heavier parent nuclei, *i.e.* the so-called superheavy nuclei ($Z_{\mathsf{P}} \geq 104$, $A_{\mathsf{P}} \gtrsim 250$), the present calculation method combined with the measured alpha-decay half-life data lead to b_α-values still lower than those listed in table 1. Since the cross sections of production of these heaviest nuclei are very low too it results very unlikely (even not practicable) to observe cluster decays of superheavy nuclei such as the synthesized by the methods currently used in. Nevertheless, a remarked effect of the 126 neutron shell closure on exotic decay half-life would be still seen if it would be possible to observe such decays. As an example, figure 6 shows for the superheavies ^{278}110 and ^{282}111 parent nuclei the calculated half-life trends for the emission of Cu and Ni isotopes. In all cases a sharp minimum in $\tau = \log T_{1/2}$ occurs whenever the number of neutrons of the daughter nucleus fills completely the 126 shell. The reason is that for an isotopic sequence of clusters from the same parent emitter the trend of half-life τ is almost totally governed by the quantum mechanical cluster penetrability through the separation, external Coulomb barrier region, which trend in turn is proportional to the quantity $F(u)/\sqrt{Q}$, $u = Q/V_{\mathsf{c}}$ (see eq. (16)). This latter is a strongly decreasing function of Q-value (see the case for $^{282}111 \rightarrow {}^{70\text{–}77}$Cu detailed in the inset graph of figure 6). Since Q is maximum when one or both decay products exhibit a structure of closed shell (mainly for neutrons) because of the greatest binding energies of these nuclei, this peak Q-value will lead ultimately to a sharp minimum in the half-life.

7 Uncertainties in calculated exotic decay half-lives

Once the choice for parametrization of the nuclear radii R_i ($i = \mathsf{P}, \mathsf{D}, \mathsf{C}$) has been done (eqs. (21)–(26)) to systematize all the existing data of partial half-life of exotic decays, the uncertainty associated to an estimated half-life value, $\delta\tau$, depends basically upon the uncertainties accompanying Q-value, δQ, and parameter g, δg (figure 3). Calculations have indicated that for heavier cluster emission cases angular momentum, ℓ, does not affect significantly the estimated half-lives. For example, when one passes from $\ell = 0$ to $\ell = 6$ in cases for ^{34}Si emission the variation in $\tau = \log T_{1/2}$ (s) is solely $\Delta\tau \approx 0.13$; for a ^{60}Cr cluster it is $\Delta\tau \approx 0.07$, and for ^{83}As it gives $\Delta\tau \approx 0.05$. Hence, we thought it unnecessary to consider such small variations in the half-life due to changes in ℓ-values. Therefore, it results that the major contributions to $\delta\tau$ should be due to δQ and δg. In this way, starting from eq. (7), and using (8), (15), and (16) all valid for $\ell = 0$, an evaluation of $\delta\tau$ can be obtained as

$$\delta\tau = \left[\left(\frac{\partial\tau}{\partial g} \right)^2 (\delta g)^2 + \left(\frac{\partial\tau}{\partial Q} \right)^2 (\delta Q)^2 \right]^{1/2} \tag{33}$$

in which

$$\left| \frac{\partial\tau}{\partial g} \right| = k_1 \sqrt{1-u}\,, \quad u = Q/V_{\mathsf{c}} \tag{34}$$

$$\left| \frac{\partial\tau}{\partial Q} \right| = \frac{1}{2Q} \left[0.4343 + \frac{k_1 u}{\sqrt{1-u}} + k_2 \left(\frac{F(u)}{\sqrt{u}} + 2\sqrt{1-u} \right) \right] , \tag{35}$$

and where

$$k_1 = 0.19\,(c-a)\,\sqrt{\mu_0 V_{\mathsf{c}}} \quad \text{and} \quad k_2 = 0.27358\,Z_{\mathsf{C}} Z_{\mathsf{D}}\,\sqrt{\mu_0/V_{\mathsf{c}}}\,. \tag{36}$$

Suppose, for instance, one uses the FRDM-mass table [48] instead of the AME03 [45] to obtain Q-value for exotic decays (electron screening always included). In this case one may consider δQ as the difference between the Q-values which come from each other mass-table, *i.e.* $\delta Q = \Delta Q = Q(\text{FRDM}) - Q(\text{AME03})$. Some representative examples of the resulting half-life uncertainties, $\delta\tau$, can be appreciated in Table 2 (5$^{\text{th}}$ column). It is seen that the $\delta\tau$-values are estimated in the range $\sim$1–3 orders of magnitude, and they result from a combination of variations in atomic mass excess and mass asymmetry of the process.

On the other hand, if one uses the mass excess and its one standard deviation error as tabulated in the AME03 mass evaluation [45] to obtain the Q-values and their associated uncertainties δQ (6^{th} and 7^{th} columns, respectively, in Table 2) the resulting half-life uncertainties drop to $\sim$1–2 orders of magnitude (8^{th} column in Table 2), and seem to increase with mass asymmetry (this is because the mass excess of the heaviest nuclei are in general less precise than that of known nuclei).

8 Exotic radioactivity of median-mass nuclei

Not only translead nuclei do (or may) disintegrate by the emission of heavy nuclear fragments of $Z_{\mathsf{C}} \geq 6$, but some median-mass parent nuclei may undergo such mode of radioactive decay as well. In fact, some reasearch works, both theoretical [3, 8, 10, 17, 53] and experimental [54, 55], were in recent past devoted to investigation of such type of decay. However, experiments have indicated to date negative results at all [54, 55].

In addition to a positive Q-value required for the process to be energetically possible, the quantity $u = Q/V_{\mathsf{c}}$ $(0 < u < 1)$ must be as great as possible, at the same time that the product $Z_{\mathsf{C}}Z_{\mathsf{D}}$ be small. These conditions are satisfactorily fulfilled in decay cases for which the daughter nucleus results around the double magic ${}^{100}_{50}$Sn and the emitted clusters may be ^{12}C, ^{16}O, ^{20}Ne, and ^{28}Si. Therefore, the parent nuclei should be proton-rich isotopes of the elements extending from Barium ($Z_{\mathsf{P}} = 56$) up to Gadolinium ($Z_{\mathsf{P}} = 64$). Hence this region of parent nuclei is being known as the transtin island of cluster emitters, in analogy to the translead cluster emitters leading to the daughter ${}^{208}_{82}$Pb nucleus.

We have applied the present calculation model to evaluate the half-life of cluster emission in transtin nuclei such as the ones mentioned above. More than fifty cases have been computed of which nearly forty ones have given $\tau = \log T_{1/2}\,(\mathrm{s}) \lesssim 28$. Results are depicted in figure 7 as Geiger-Nuttall-like plots, in complete analogy to what was observed very early in alpha decay [56]. The apparent quite linear trend of decreasing of τ with increasing Q-value showed in figure 7 is a direct consequence of the formalism described by eqs. (7)–(13). In fact, for a given cluster to be emitted from parent nuclei of the same isotopic sequence the quantities τ_0, $c - a$, μ_0, V_{c}, and, therefore, k_1 and k_2 as given by eq. (36) do not vary appreciably, so that the half-life can be expressed as

$$\tau = \tau_0 + k_1\sqrt{1-u} + k_2 F(u)/\sqrt{u}\,, \quad u = Q/V_{\mathsf{c}}\,. \tag{37}$$

Now, it is sufficient to expand (37) about $\overline{u} = \langle Q/V_{\mathsf{c}}\rangle$ keeping only the first two terms in the expansion. Here, $\overline{u}$ is the average value of the Q/V_{c}-values of the different decay cases in an isotopic sequence of parent nuclei. In this way, the half-lives follow the approximate linear trends obtained by

$$\tau(Q) \approx \tau(\overline{u}) + \frac{\tau'(\overline{u})}{V_{\mathsf{c}}}\,(Q - \langle Q\rangle)\ . \tag{38}$$

For the emission cases $^{114\text{–}120}$Ba $\to$ ^{12}C, for instance, one obtains

$$\log T_{1/2}(\mathrm{s}) = \tau \approx 68.53 - 3.15\,Q\,. \tag{39}$$

Despite the promising decay case ^{114}Ba $\to$ ^{12}C (Q-value $=$ 19.05 MeV), which shows the lowest predicted half-life-value of $T_{1/2} = 4.7\times10^9$ s, careful experiments conducted to search for this decay process have led to the conclusion of nonobservation of ^{12}C decay of ^{114}Ba isotope [54].

9 Conclusion

The radioactive decay by the emission of nuclear fragments heavier than the alpha particle is a process firmly established from both experimental and theoretical points of view. Investigations on such exotic decays during the last thirty years or so have indicated a number of cases of clusters (^{14}C–^{34}Si) emitted from translead (Fr–Cm) parent nuclei of extremely low (5×10^{-17}–4×10^{-9}) branching ratio relative to alpha decay. All current models that have been developed to give a quantitative description of this rare nuclear process are based on the quantum-mechanical tunneling mechanism of penetration through a potential barrier, and they have shown that this spontaneous nuclear break-up may also occur in heavier nuclei and median-mass, transtin nuclei as well.

Like in alpha decay and ordinary fission processes, cluster radioactivity is a manifestation of the nuclear shell structure, and the most likely observed cases have been those where the product nuclei exhibit a neutron or proton (or both) shell closure. The phenomenon can be described quite similar to alpha decay, although some remarked differences there exist such as *i*) preformation probability of a cluster at the nuclear surface 4–10 orders of magnitude smaller than that for an alpha particle; *ii*) difficulties in detecting these rare modes of decay in view of the expected extremely small branching ratio relative to alpha decay; *iii*) large uncertainties ($\sim$1–2 orders of magnitude) to predicted half-lives for new cases of cluster decay from the current models. However, Geiger-Nuttall-like plots for different heavy-ion emissions emerge nicely in a quite complete analogy to what was very early observed in alpha decay.

To conclude, it would be rewarding to see detected and measured in a near future other cases for *natural* cluster radioactivity such as ^{26}Ne from ^{232}Th ($b_\alpha \sim 2 \times 10^{-12}$) and the intriguing radioactive disintegration of ^{34}Si from ^{238}U for which case the branching ratio relative to alpha decay has been computed as 10^{-13}–10^{-11}. The authors anticipate seeing results confirmed.

References

[1] Poenaru D N, Ivascu M, Săndulescu A and Greiner W 1985 Atomic nuclei decay modes by spontaneous emission of heavy ions *Phys. Rev.* C **32** 572

[2] Shi Yi-Jin and Swiatecki W J 1985 Estimates of radioactive decay by the emission of nuclei heavier than α-particles *Nucl. Phys.* A **438** 450

[3] Poenaru D N, Schnabel D, Greiner D, Mazilu D and Gherghescu R 1991 Nuclear lifetimes for cluster radioactivities *At. Data Nucl. Data Tables* **48** 231

[4] Zamyatnin Yu S, Mikheev V L, Tretyakova S P , Furman V I, Kadmenskĩi S G, and Chuvil'skĩi Yu M 1990 Cluster radioactivity: progress and perspectives; experiment and theory *Fiz. Elem. Chas-tits At. Yadra* **21** 537
Zamyatnin Yu S, Mikheev V L, Tretyakova S P , Furman V I, Kadmenskĩi S G, and Chuvil'skĩi Yu M 1990 *Sov. J. Part. Nucl.* **21** 231

[5] Gonçalves M and Duarte S B 1993 Effective liquid drop description for the exotic decay of nuclei *Phys. Rev.* C **48** 2409

[6] Ardisson G and Hussonnois M 1995 Radiochemical investigations of cluster radioactivities *Radiochim. Acta* **70/71** 123

[7] Poenaru D N (ed) 1996 *Nuclear Decay Modes* (Bristol: Institute of Physics Publishing) chapters 6–9

[8] Duarte S B, Tavares O A P, Guzmán F, Dimarco A, Garcia F, Rodriguez O and Gonçalves M 2002 Half-lives for proton emission, alpha-decay, cluster radioactivity, and cold fission processes calculated in a unified theoretical framework *At. Data Nucl. Data Tables* **80** 235

[9] Tretyakova S P, Ogloblin A A and Pik-Pichak G A 2003 The present state of cluster radioactivity research *Phys. Atom. Nucl.* **66** 1618

[10] Kuklin S N, Adamian G G and Antonenko N V 2005 Spectroscopic factors and cluster decay half-lives of heavy nuclei *Phys. Rev.* C **71** 014301

[11] Tavares O A P, Roberto L A M and Medeiros E L 2007 Radioactive decay by the emission of heavy nuclear fragments *Phys. Scr.* **76** 375

[12] Bonetti R and Guglielmetti A 2007 Cluster radioactivity: an overview after twenty years *Roman. Rep. Phys* **59** 301

[13] Ni D, Ren Z, Dong T and Xu C 2008 Unified formula of half-lives for α decay and cluster radioactivity *Phys. Rev.* C **78** 044310

[14] Poenaru D N, Gherghescu R A and Greiner W 2011 Single universal curve for cluster radioactivities and α decay *Phys. Rev.* C **83** 014601

[15] Blendowske R, Fliessbach T and Walliser H 1996 Many-body approach to alpha and cluster radioactivity in *Nuclear Decay Modes* (Poenaru D N Editor) (Bristol: Institute of Physics Publishing) Chapter 7

[16] Warda M and Robledo L M 2011 Microscopic description of cluster radioactivity in actinide nuclei *Phys. Rev.* C **84** 044608

[17] Santhosh K P, Biju R K and Sahadevan S 2010 Cluster formation probability in the trans-tin and trans-lead nuclei *Nucl. Phys.* A **833** 38

[18] Rose H J and Jones G A 1984 A new kind of natural radioactivity *Nature* **307** 245

[19] Aleksandrov D V, Belyatskĩi A F, Glukhov Yu A, Nikol'skĩi E Yu, Novatskĩi B G, Ogloblin A A and Stepanov D N 1984 Observation of the spontaneous emission of ^{14}C nuclei from ^{223}Ra *Pis. Zh. Eksp. Teor. Fiz.* **40** 152
Aleksandrov D V, Belyatskĩi A F, Glukhov Yu A, Nikol'skĩi E Yu, Novatskĩi B G, Ogloblin A A and Stepanov D N 1984 *Sov. Phys. - JETP Lett.* **40** 909

[20] Gales S, Hourani E, Hussonnois M, Schapira J P, Stab L and Vergnes M 1984 Exotic nuclear decay of ^{223}Ra by emission of ^{14}C nuclei *Phys. Rev. Lett.* **53** 759

[21] Price P B, Stevenson J D, Barwick S W and Ravn H L 1985 Discovery of radioactive decay of ^{222}Ra and ^{224}Ra by ^{14}C emission *Phys. Rev. Lett.* **54** 297

[22] Kutschera W, Ahmad I, Armato III S G, Friedman A M, Gindler J E, Henning W, Ishic T, Paul M and Rehm K E 1985 Spontaneous ^{14}C emission from ^{223}Ra *Phys. Rev.* C **32** 2036

[23] Guglielmetti A, Faccio D, Bonetti R, Shishkin S V, Tretyakova S P, Dmitriev S V, Ogloblin A A, Pik-Pickak G A, van der Meulen N P, Steyn G F, van der Walt T N, Vermeulen C and McGee D 2008 Carbon radioactivity of ^{223}Ac and a search for nitrogen emission *J. Phys.: Conf. Ser.* **111** 012050

[24] de Carvalho H G, Martins J B, de Souza I O and Tavares O A P 1975 Emissão espontânea de íons pesados pelo urânio [Spontaneous emission of heavy ions from Uranium] *An. Acad. Brasil. Ciênc.* **47** 567; see also: de Carvalho H G, Martins J B, de Souza I O and Tavares O A P 1976 Spontaneous emission of heavy ions from Uranium *Chem. Abstr.* **85** 441 (entry No. 85: 100326j)

[25] de Carvalho H G, Martins J B, de Souza I O and Tavares O A P 1976 Spontaneous emission of heavy-ions from uranium *An. Acad. Brasil. Ciênc.* **48** 205

[26] de Souza I O 1975 *MSc Thesis* Centro Brasileiro de Pesquisas Físicas - CBPF (Rio de Janeiro)

[27] Tavares O A P 1978 *Doctoral Thesis* Centro Brasileiro de Pesquisas Físicas - CBPF (Rio de Janeiro)

[28] de Carvalho H G, Martins J B and Tavares O A P 1986 Radioactive decay of radium and radon isotopes by ^{14}C emission *Phys. Rev.* **34** 2261

[29] Săndulescu A and Greiner W 1977 Mass asymmetry in fission, fusion and mass-transfer due to fragmentation in valleys *J. Phys. G: Nucl. Part. Phys.* **3** L189

[30] Săndulescu A, Lustig H J, Hahn J and Greiner W 1978 High mass-asymmetry distributions of fissionning nuclei *J. Phys. G: Nucl. Part. Phys.* **4** L279

[31] Săndulescu A, Poenaru D N and Greiner W 1980 New type of decay of heavy nuclei intermediate between fission and α decay *Fiz. Elem. Chas-tits Yadra* **11** 1334
Săndulescu A, Poenaru D N and Greiner W 1980 *Sov. J. Part. Nucl.* **11** 528

[32] Poenaru D N, Ivascu M, Săndulescu A and Greiner W 1984 Spontaneous emission of heavy clusters *J. Phys. G: Nucl. Part. Phys.* **10** L183

[33] Poenaru D N, Greiner W, Depta K, Ivascu M, Mazilu D and Săndulescu A 1986 Calculated half-lives and kinetic energies for spontaneous emission of heavy ions from nuclei *At. Data Nucl. Data Tables* **34** 423

[34] Guglielmetti A, Bonetti R, Poli G, Price P B, Westphal A J, Janas Z, Keller H, Kirchner R, Klepper O, Piechaczek A, Roecki E, Schmidt K, Plochocki A, Szeripo J and Blank B 1995 Identification of the new isotope ^{114}Ba and search for its α and cluster radioactivity *Phys. Rev.* C **52** 740

[35] Kuklin S N, Adamian G G and Antonenko N V 2005 Spectroscopic factors and barrier penetrabilities in cluster radioactivity *Phys. Atom. Nucl.* **68** 1443

[36] Hourani E, Hussonnois M and Poenaru D N 1989 Radioactivities by light fragment (C, Ne, Mg) emission *Ann. Phys.* (Paris) **14** 311

[37] Poenaru D N, Gherghescu R A and Greiner W 2011 Heavy-particle radioactivity of superheavy nuclei *Phys. Rev. Lett.* **107** 062503

[38] Poenaru D N, Gherghescu R A and Greiner W 2012 Cluster decay of superheavy nuclei *Phys. Rev.* C **85** 034615

[39] Tavares O A P, Medeiros E L and Terranova M L 2005 Alpha decay half-life of bismuth isotopes *J. Phys. G: Nucl. Part. Phys.* **31** 129

[40] Tavares O A P, Terranova M L and Medeiros E L 2006 New evaluation of alpha decay half-life of ^{190}Pt isotope for the Pt-Os dating system *Nucl. Instrum. Methods Phys. Res.*B **243** 256

[41] Tavares O A P and Medeiros E L 2011 Natural and artificial alpha radioactivity of platinum isotopes *Phys. Scr.* **84** 045202

[42] Medeiros E L, Rodrigues M M N, Duarte S B and Tavares O A P 2007 Systematics of half-lives for proton radioactivity *Eur. Phys. J.* A **34** 417

[43] Tavares O A P and Medeiros E L 2010 Proton radioactivity: the case for $^{53\mathrm{m}}$Co proton-emitter isomer *Eur. Phys. J.* A **45** 57

[44] Duarte S B and Gonçalves M G 1996 Effective inertial coefficient for the dinuclear regime of the exotic decay of nuclei *Phys. Rev.* C **53** 2309

[45] Audi G, Bersillon O, Blachot J and Wapstra A H 2003 The NUBASE evaluation of nuclear and decay properties *Nucl. Phys.* A **729** 3

[46] Huang K-N, Aoyagi M, Chen M H, Crasemann B and Mark H 1976 Neutral-atom electron binding energies from relaxed-orbital relativistic Hartree-Fock-Slater calculations $2 \leq Z \leq 106$ *At. Data Nucl. Data Tables* **18** 243

[47] Myers W D 1977 *Droplet Model of Atomic Nuclei* (New York: Plenum)

[48] Möller P, Nix J R, Myers W D and Swiatecki W J 1995 Nuclear ground-state masses and deformations *At. Data Nucl. Data Tables* **59** 185

[49] Dobaczewski J, Nazarewicz W and Werner T R 1996 Neutron radii and skins in the Hartree-Fock-Bogoliubov calculations *Z. Phys.* A **354** 27

[50] Audi G and Meng W 2011 Atomic mass adjustment *Private Communication* April 2011

[51] Tretyakova S P, Mikheev V L, Ponomarenko V A, Golovchenko A N, Ogloblin A A and Shigin V A 1994 Cluster decay of ^{236}U *JETP Lett.* **59** 394

[52] Ronen Y 1991 Significance of the light clusters in exotic nuclear decay *Phys. Rev.* C **44** R594

[53] Poenaru D N, Greiner W and Cherghescu R 1993 New island of cluster emitters *Phys. Rev.* C **47** 2030

[54] Guglielmetti A, Bonetti R, Poli G, Collatz R, Hu Z, Kirchner R, Roeckl E, Gunn N, Price P B, Weaver B A, Westphal A and Szerypo J 1997 Nonobservation of ^{12}C cluster decay of ^{114}Ba *Phys. Rev.* C **56** R2912

[55] Bernabei R, Belli P, Cappella F, Montecchia F, Nozzoli F, d'Angelo A, Incicchitti A, Prosperi D, Cerulli R, Dai C J, He H L, Huang H H, Ma J M, Ye Z P and Tretyak V I 2005 A search for spontaneous emission of heavy clusters in the ^{127}I nuclide *Eur. Phys. J.* A **24** 51

[56] Geiger H and Nuttall J M 1911 The ranges of the α-particles from various radioactive substances and a relation between range and period of transformation *Phil. Mag.* **22** 613; Geiger G 1922 Reichweitemessungen an α-strahlen *Z. Phys.* **8** 45

Table 1 - A sample of calculated half-life values for radioactive decay of heaviest actinide parent nuclei by the emission of massive ($Z_c \geq 14$) nuclear fragments.

Parent nucleus			Emitted cluster		Daughter nucleus		Mass asymmetry[a]	Q-value[b]	Half-life values, $\tau_c = \log T_{1/2}$ (s)			Branching to α-decay[d]
El	Z_P	A_P	Z_c	N_c	Z_D	N_D	η	(MeV)	This work	Ref. [3]	Ref. [8]	$\log b_\alpha$
U	92	238	14	20	78	126	0.714	86.06[c]	30.02	——	——	−12.87
Np	93	236	14	18	79	125	0.729	88.47	27.58	——	26.71	−12.11
		237	14	18	79	126	0.730	87.96	28.16	30.0	26.99	−14.33
Pu	94	238	14	18	80	126	0.731	91.45	25.37	26.1	24.43	−15.93
		239	14	20	80	127	0.715	91.09	26.84	29.0	25.75	−14.96
		240	14	20	80	126	0.717	91.29	26.52	27.4	25.40	−15.20
Am	95	241	14	18	81	128	0.734	90.92	27.50	28.9	26.59	−17.37
			14	20	81	126	0.718	94.19	24.53	25.8	23.37	−14.40
		243	14	20	81	128	0.720	91.04	28.34	29.9	27.25	−16.97
Cm	96	240	14	18	82	126	0.733	97.82	20.96	21.2	19.90	−14.59
			14	20	82	124	0.717	95.74	24.40	25.1	23.29	−18.03
		242	14	18	82	128	0.736	93.88	25.42	26.0	——	−18.27
			14	20	82	126	0.719	96.78	23.00	23.5	21.81	−15.85
		243	14	20	82	127	0.720	95.02	25.03	27.0	23.87	−16.07
Cf	98	252	18	28	80	126	0.635	127.04	26.53	26.5	23.81	−18.60
Es	99	252	20	28	79	125	0.619	142.63	26.08	27.6	22.77	−18.36
		254	18	28	81	127	0.638	128.81	26.41	28.2	23.67	−19.03
			20	30	79	125	0.606	142.69	26.44	27.9	22.96	−19.06
Md	101	258	20	30	81	127	0.612	148.40	24.44	25.2	20.79	−17.79
No	102	259	20	29	82	128	0.622	150.53	24.00	——	20.41	−20.33
			20	30	82	127	0.614	151.69	23.13	23.3	19.42	−19.46

[a] This is defined by $\eta = 1 - 2A_C/A_P$.

[b] Screening effects included (see equation (20)).

[c] Assuming a mass excess of −18.54 MeV for ^{204}Pt isotope according to the droplet model by Möller *et al.* [48].

[d] This is given by $\log b_\alpha = \tau_\alpha - \tau_c$ where τ_α is the decimal logarithm of the measured partial alpha-decay half-life as tabulated in [45], and τ_c is the corresponding entry in the 10th column.

Table 2 - Examples of evaluation of half-life uncertainties in exotic radioactivity.

Decay case	Q-value[a] (MeV)				Q-value[a] (MeV)		
	FRDM [48]	AME03 [45]	$\delta Q = \Delta Q$	$\delta\tau$	AME03 [45]	δQ[b]	$\delta\tau$
^{228}Th $\rightarrow$ ^{20}O + ^{208}Pb	46.06	44.87	1.19	2.3	44.87	0.003	0.8
^{240}Pu $\rightarrow$ ^{34}Si + ^{206}Hg	91.41	91.29	0.12	1.3	91.29	0.024	1.3
^{259}No $\rightarrow$ ^{50}Ca + ^{209}Pb	150.27	151.69	1.42	2.1	151.69	0.100	1.6
^{282}Rg $\rightarrow$ ^{73}Ni + ^{209}Bi	224.13	224.76	0.63	2.0	224.76	0.939	2.1
^{291}115 $\rightarrow$ ^{85}Br + ^{206}Hg	279.12	281.36	2.24	2.7	281.36	0.890	2.1

[a] Screening effects included (see equation (20)).

[b] $\delta Q = [(\delta\,\Delta M_{\mathsf{P}})^2 + (\delta\,\Delta M_{\mathsf{D}})^2 + (\delta\,\Delta M_{\mathsf{C}})^2]^{1/2}$ where the $\delta\,\Delta M\,'$s are the 1σ errors to the mass excess values as tabulated in the AME03 [45].

Figure Captions

Fig. 1 Illustrating the one-dimensional potential barrier for three cases of cluster radioactivity. The shaded area emphasizes the overlapping barrier region *a*–*c* (where the cluster is being formed). The region of the external barrier *c*–*b* comprises the Coulomb plus centrifugal (for cases of $\ell \neq 0$) contributions to the barrier. Note the differences when one passes from case a) to c).

Fig. 2 Reduced, equivalent liquid drop nuclear radius ($r_0 = R/A^{1/3}$) to the average equivalent root-mean-squares radius of the proton and neutron density distributions following the finite-range droplet model by Möller *et al.* [48]. Different symbols refer to different types of nuclei as indicated.

Fig. 3 Values of parameter g obtained semiempirically as a function of mass asymmetry, η, for all cases of cluster radioactivity observed to date. Symbols represent different cluster emission cases as indicated (parent nuclei are shown straight in front of each emitted cluster). The dashed line represents the average value ($\overline{g} = 0.349 \pm 0.021$), and the shaded area its uncertainty to 1.7σ.

Fig. 4 Reduced half-life, $\tau_\mathsf{r} \equiv \tau_2^\mathsf{coul}$ (defined by eqs. (30) and (31)) plotted against Coulomb parameter z (as given by definition (30)) for all cases of cluster radioactivity observed to date. Symbols represent experimental reduced half-lives, $\tau_\mathsf{r}^\mathsf{e}$, for cluster emission cases indicated in the same way as shown in figure 3. τ_r-values have been obtained by using the average $\overline{g}$-value shown in figure 3. The straight line $\tau_\mathsf{r}^\mathsf{c} = 0.27358z$ gives the reduced calculated half-life values according to the present methodology. The left inset graph shows the distribution of the difference $\Delta\tau = \tau^\mathsf{c} - \tau^\mathsf{e} = \tau_\mathsf{r}^\mathsf{c} - \tau_\mathsf{r}^\mathsf{e}$ between calculated and experimental half-life values which is seen normally centered at $\Delta\tau = 0$ with standard deviation $\sigma = 0.818$ (80% of cases are of $|\Delta\tau| \leq 1$). The right inset graph shows the range where the $\tau_\mathsf{r}^\mathsf{c}$-values for cases of eventual cluster emission from superheavy parent nuclei would be located; few examples are: □, $Z_\mathsf{p} = 104$; △, $Z_\mathsf{p} = 109$; ▽, $Z_\mathsf{p} = 112$; ○, $Z_\mathsf{p} = 115$ (full circles represent observed cluster emission cases of $87 \leq Z_\mathsf{p} \leq 96$).

Fig. 5 **a)** Average nuclear binding energy per deuteron-plus-triton, $\overline{B}_\mathsf{d+t}$ (eq. (32)), compared to **b)** average nuclear binding energy per nucleon, $\overline{B}_\mathsf{p+n}$, for intermediate-mass and less massive neutron-rich nuclei. The numbers near the broken lines are the atomic numbers of the isotopic sequences, and those near the vertical arrows indicate the neutron shell closure.

Fig. 6 Partial cluster decay half-life plotted against mass number of the emitted cluster for the decay cases $^{278}110 \rightarrow$ Ni, Cu (part a) and $^{282}111 \rightarrow$ Cu (part b). Data points are calculated values following the present calculation model. Note in all cases the clear effect caused by the 126 neutron shell closure of the daughter nucleus. The inset graph shows the variation of Q-value and the quantity $F(u)Q^{-1/2}$ (eq. (17)) with mass number of the daughter nucleus, A_D, for the emission cases $^{282}111 \rightarrow ^{71-77}$Cu.

Fig. 7 Geiger-Nuttall-like plots for radioactive decay cases of median-mass parent nuclei: $^{114-120}$Ba $\rightarrow$ ^{12}C (●), $^{114-119}$Ba $\rightarrow$ ^{16}O (○), $^{119-124}$Ce $\rightarrow$ ^{16}O (■), $^{124-127}$Nd $\rightarrow$ ^{16}O (▲), $^{119-121}$Ce $\rightarrow$ ^{20}Ne (□), $^{124-126}$Nd $\rightarrow$ ^{20}Ne (△), $^{128-132}$Sm $\rightarrow$ ^{24}Mg (▼), and $^{128-132}$Sm $\rightarrow$ ^{28}Si (▽). Points represent calculated half-life data following the methodology of the present work, and the lines are to guide the eyes. All mass excess values are from the 2003 mass evaluation by Audi *et al.* [45].

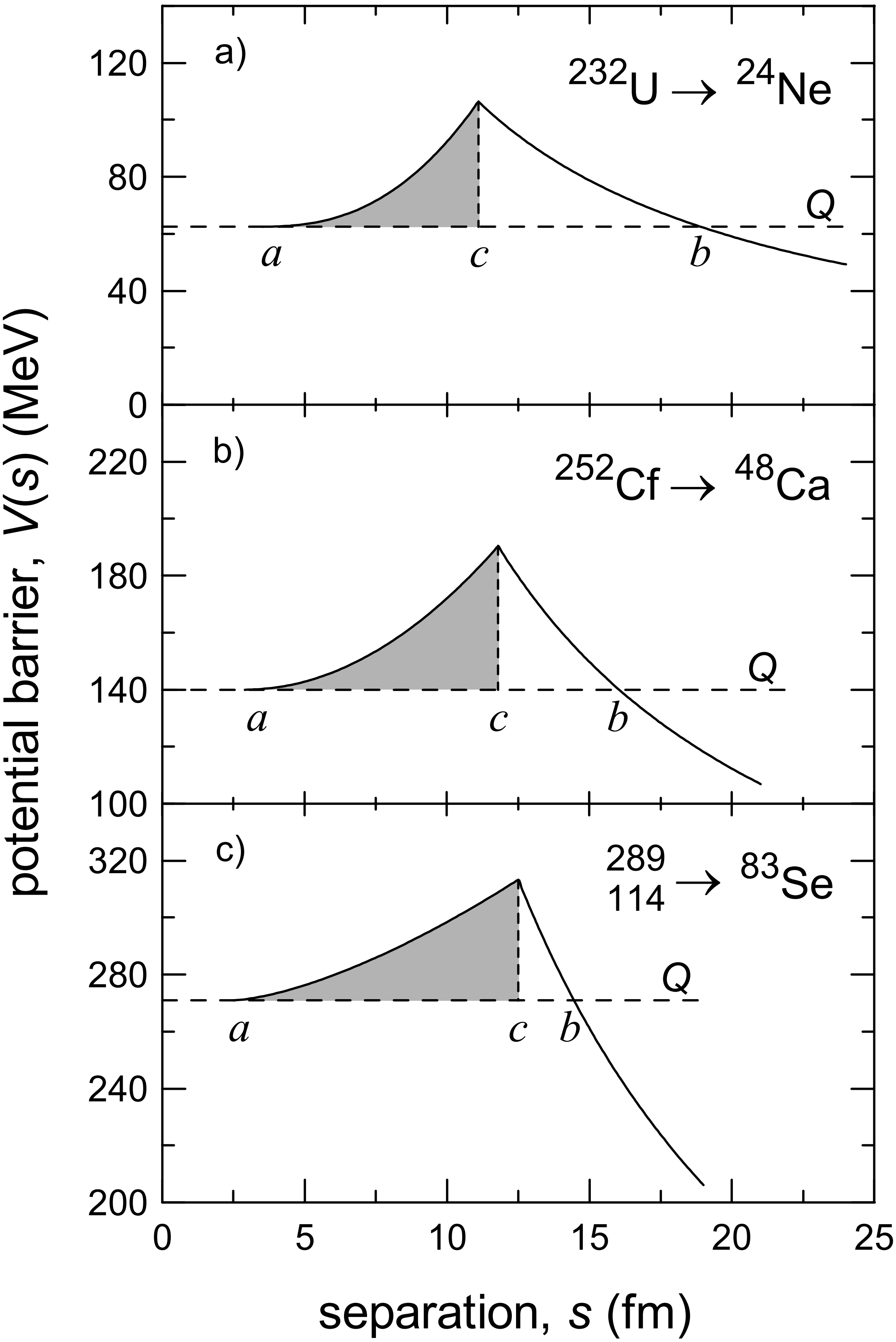
a)
$^{232}U \rightarrow {}^{24}Ne$
Q
a
c
b
b)
$^{252}Cf \rightarrow {}^{48}Ca$
Q
a
c
b
c)
$^{289}_{114} \rightarrow {}^{83}Se$
Q
a
c
b
potential barrier, V(s) (MeV)
separation, s (fm)
0
40
80
120
100
140
180
220
200
240
280
320
0
5
10
15
20
25

Fig. 1

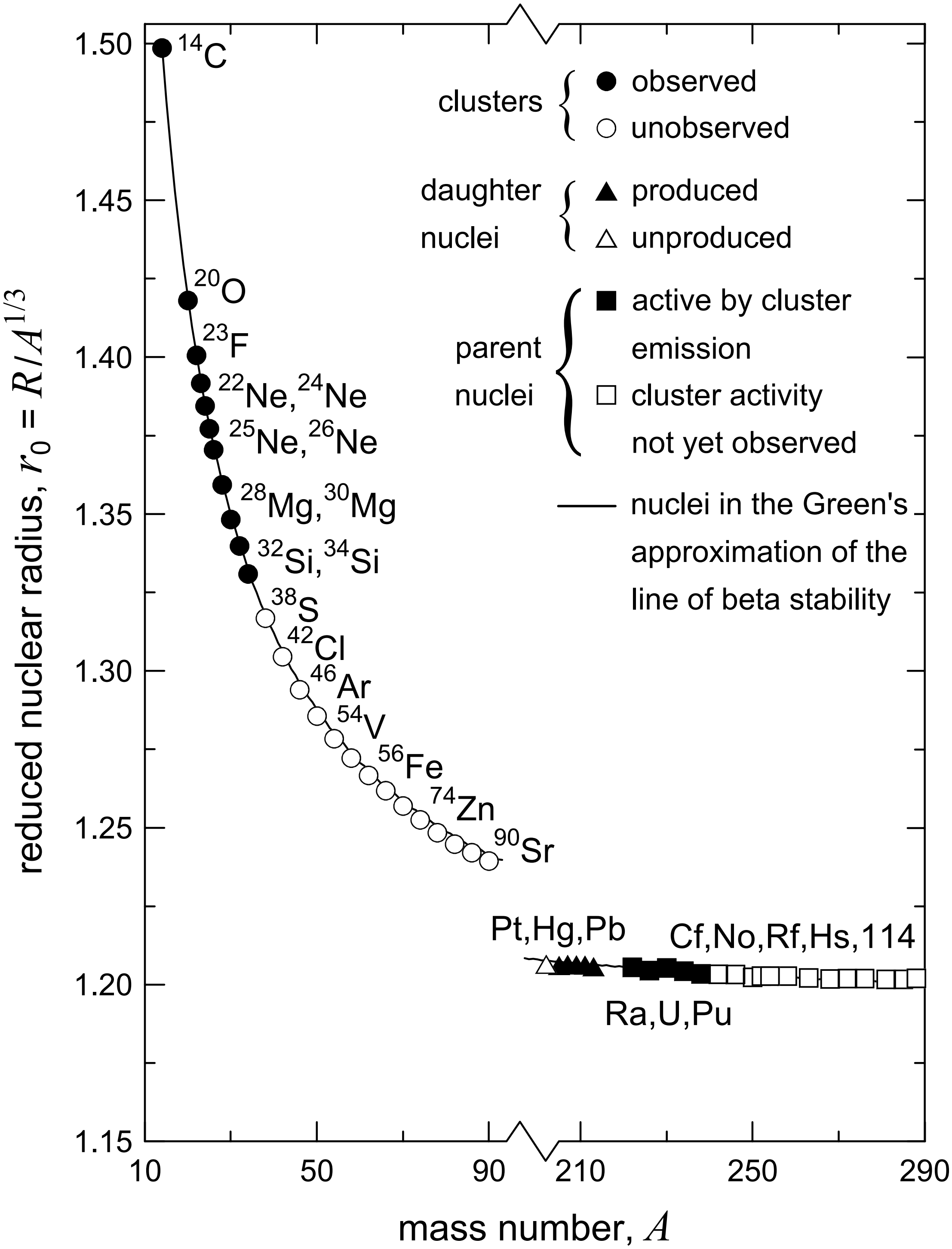

1.50
1.45
1.40
1.35
1.30
1.25
1.20
1.15
10
50
90
210
250
290
reduced nuclear radius, $r_0 = R/A^{1/3}$
mass number, A
^{14}C
^{20}O
^{23}F
^{22}Ne,^{24}Ne
^{25}Ne,^{26}Ne
^{28}Mg,^{30}Mg
^{32}Si,^{34}Si
^{38}S
^{42}Cl
^{46}Ar
^{54}V
^{56}Fe
^{74}Zn
^{90}Sr
Pt,Hg,Pb
Cf,No,Rf,Hs,114
Ra,U,Pu
clusters
observed
unobserved
daughter nuclei
produced
unproduced
parent nuclei
active by cluster emission
cluster activity not yet observed
nuclei in the Green's approximation of the line of beta stability

Fig. 2

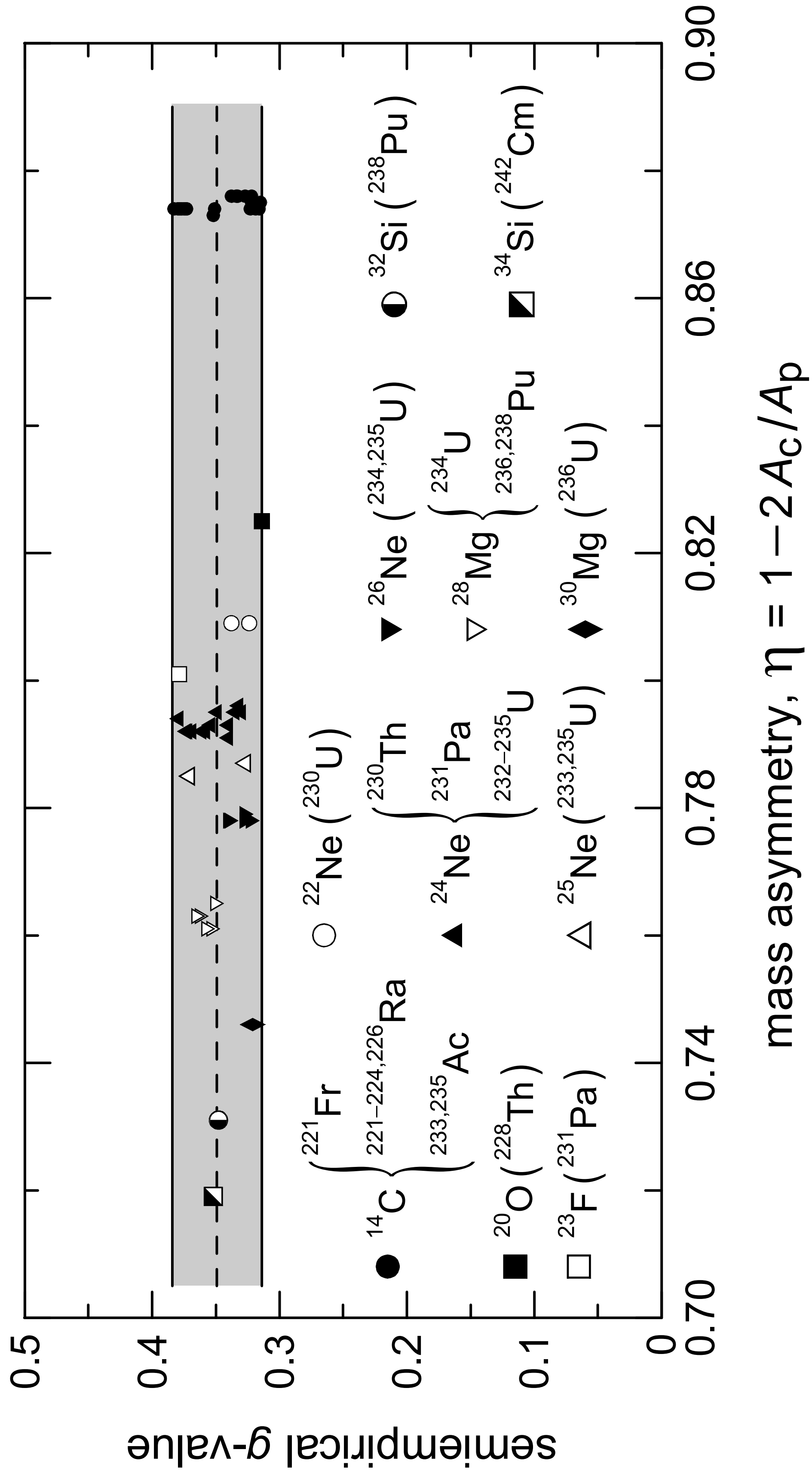
semiempirical g-value
0.5
0.4
0.3
0.2
0.1
0
0.70
0.74
0.78
0.82
0.86
0.90
mass asymmetry, η = 1 − 2 Ac / Ap
14C { 221Fr, 221−224,226Ra, 233,235Ac }
20O (228Th)
23F (231Pa)
22Ne (230U)
24Ne { 230Th, 231Pa, 232−235U }
25Ne (233,235U)
26Ne (234,235U)
28Mg { 234U, 236,238Pu }
30Mg (236U)
32Si (238Pu)
34Si (242Cm)

Fig. 3

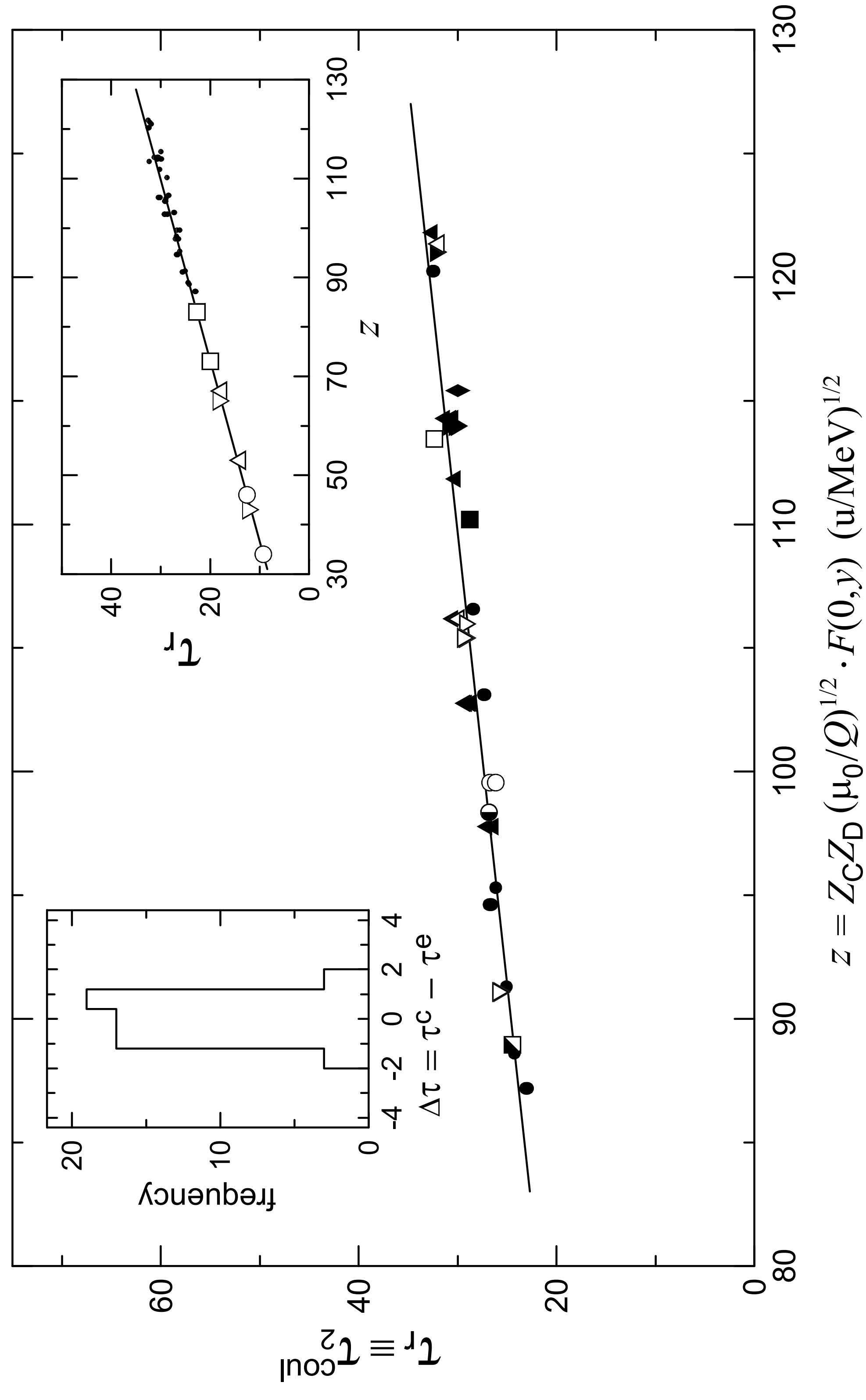
$z = Z_C Z_D (\mu_0/Q)^{1/2} \cdot F(0,y)$ (u/MeV)$^{1/2}$
$\tau_r \equiv \tau^2_{coul}$
frequency
$\Delta\tau = \tau^c - \tau^e$
τ_r
z

Fig. 4

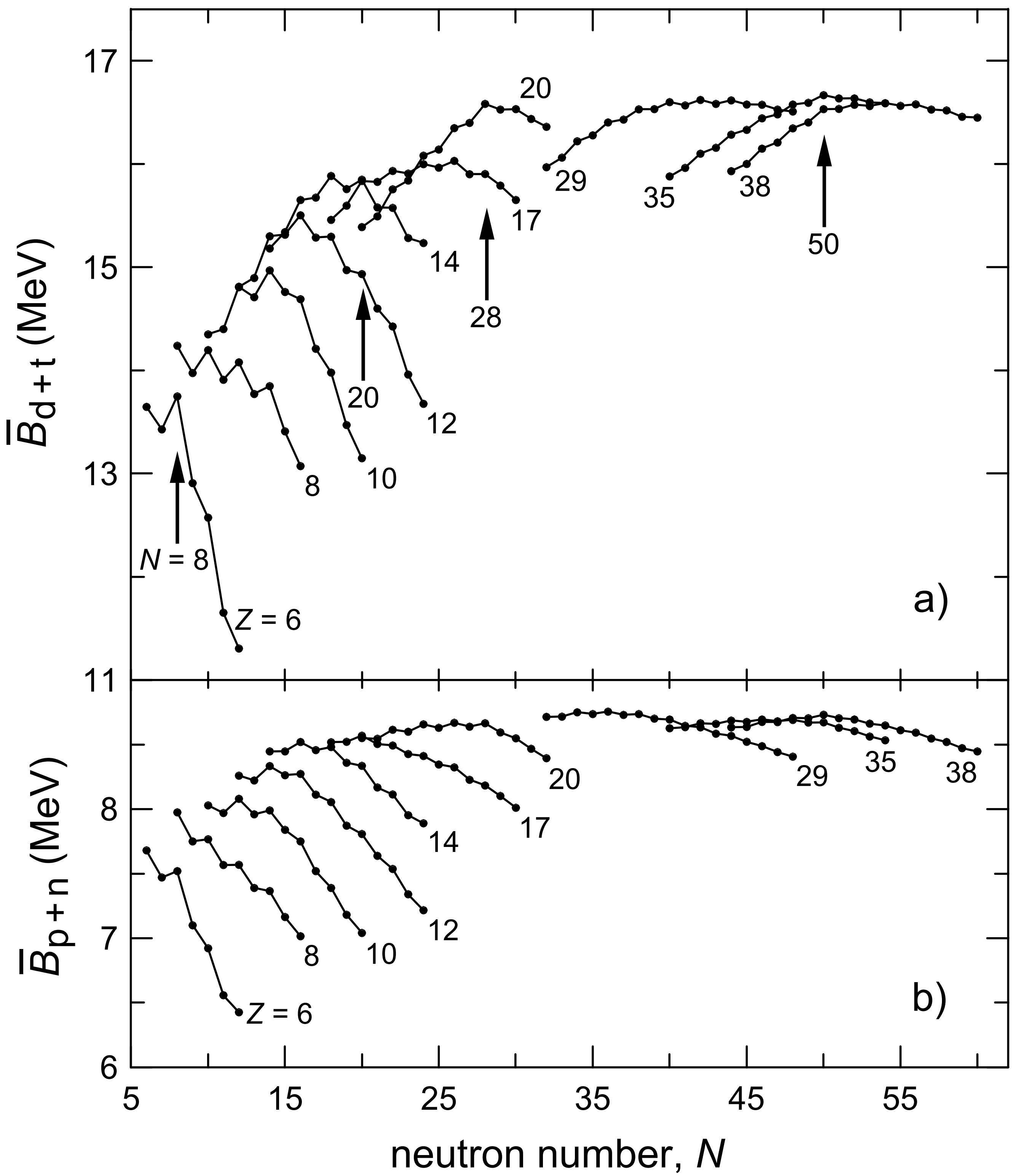

17
15
13
11
$\bar{B}_{d+t}$ (MeV)
20
29
35
38
17
14
12
10
8
28
50
20
N = 8
Z = 6
a)
8
7
6
$\bar{B}_{p+n}$ (MeV)
20
29
35
38
17
14
12
10
8
Z = 6
b)
5
15
25
35
45
55
neutron number, N

Fig. 5

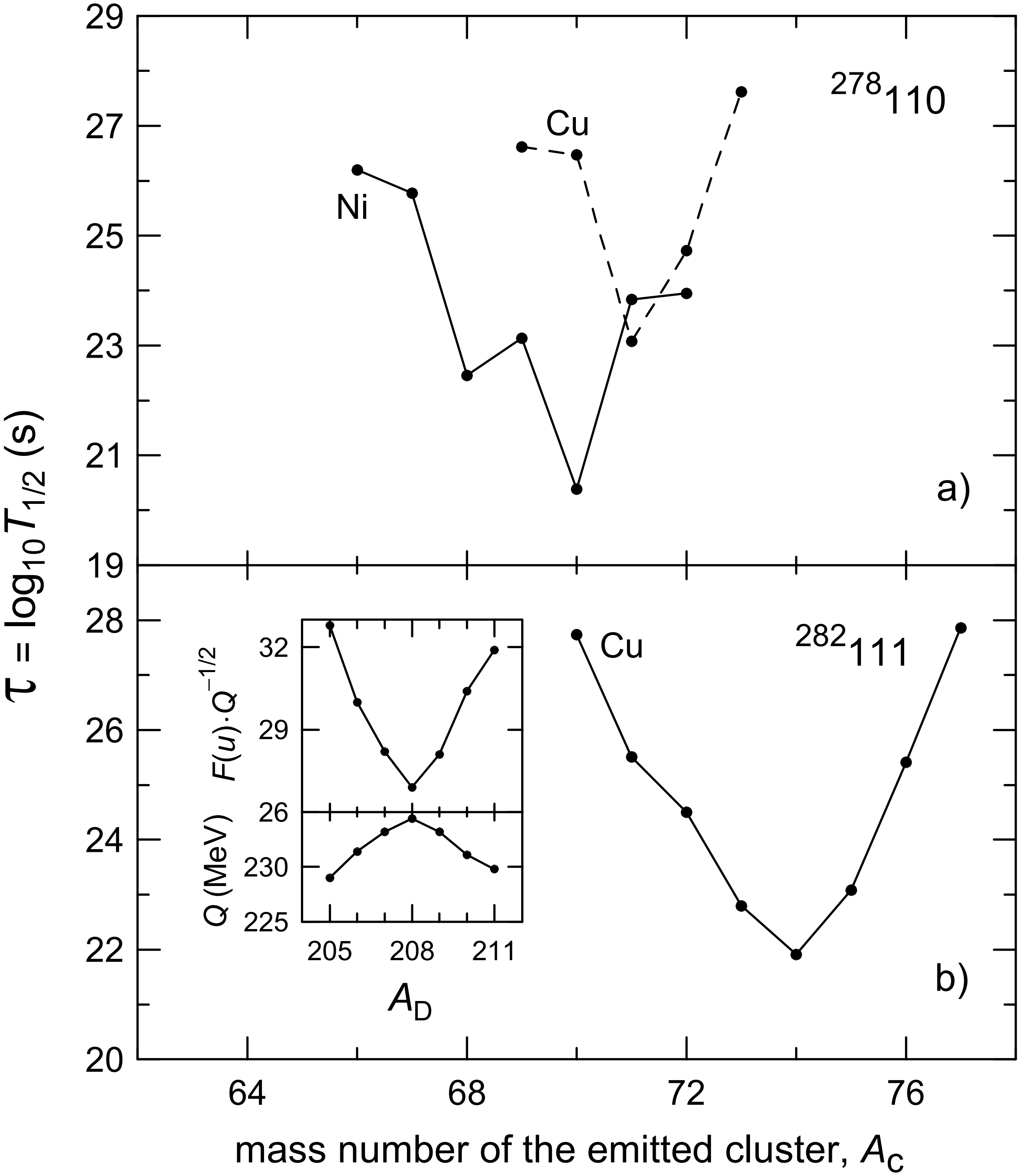
29
27
25
23
21
19
28
26
24
22
20
$^{278}110$
Cu
Ni
a)
Cu
$^{282}111$
b)
32
29
26
230
225
205
208
211
$F(u)\cdot Q^{-1/2}$
Q (MeV)
A_D
$\tau = \log_{10} T_{1/2}$ (s)
64
68
72
76
mass number of the emitted cluster, A_c

Fig. 6

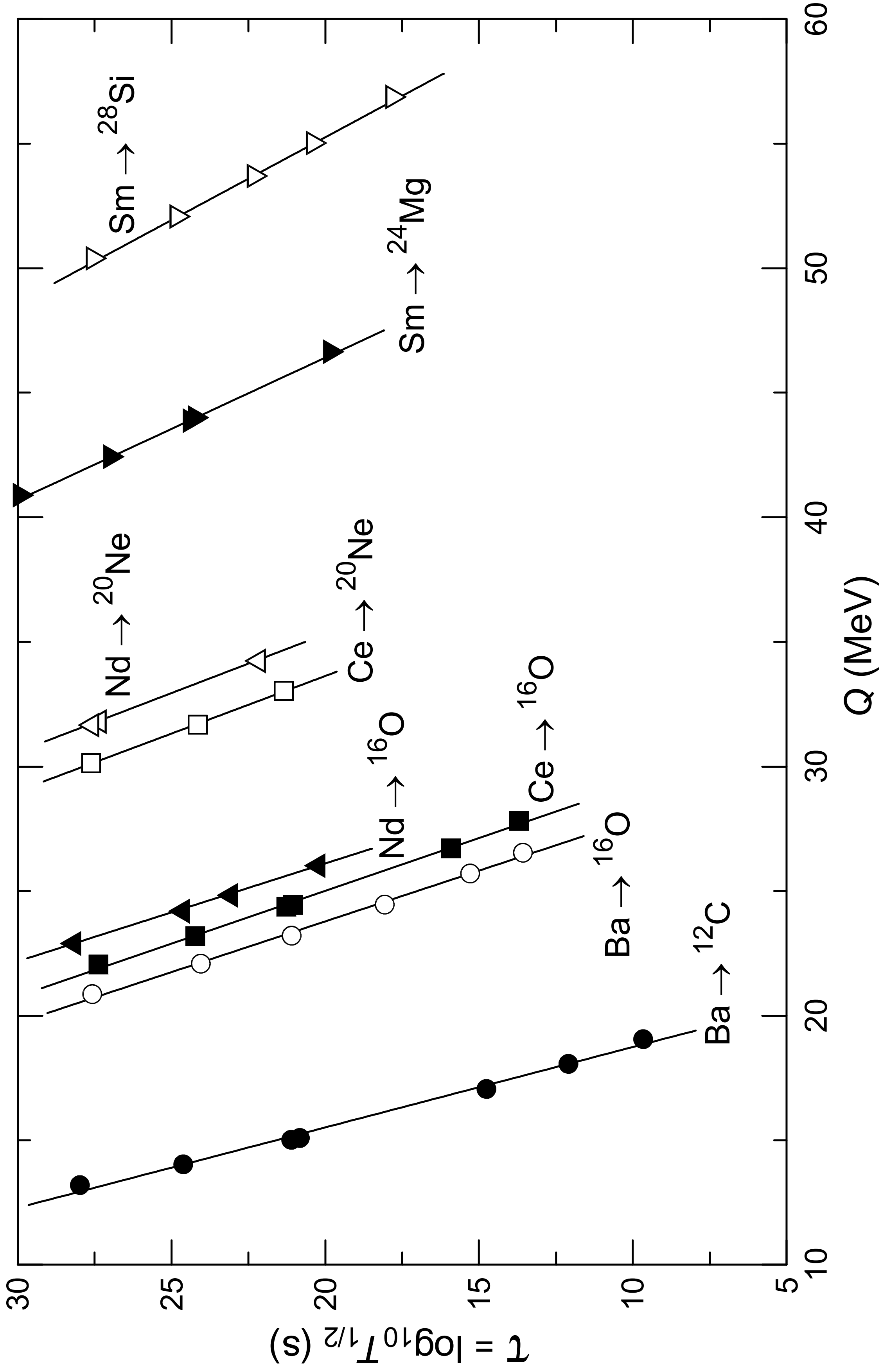
Sm → ^{28}Si
Sm → ^{24}Mg
Nd → ^{20}Ne
Ce → ^{20}Ne
Nd → ^{16}O
Ce → ^{16}O
Ba → ^{16}O
Ba → ^{12}C
Q (MeV)
τ = log$_{10}$T$_{1/2}$ (s)
10
20
30
40
50
60
5
10
15
20
25
30

Fig. 7

NOTAS DE FÍSICA é uma pré-publicação de trabalho original em Física.
Pedido de cópias desta publicação deve ser enviado aos autores ou ao:

Centro Brasileiro de Pesquisas Físicas
Área de Publicações
Rua Dr. Xavier Sigaud, 150 – 4º andar
22290-180 – Rio de Janeiro, RJ
Brasil
E-mail: socorro@cbpf.br/valeria@cbpf.br
http://www.biblioteca.cbpf.br/index_2.html

NOTAS DE FÍSICA is a preprint of original unpublished works in Physics.
Request for copies of this report should be addressed to:

Centro Brasileiro de Pesquisas Físicas
Área de Publicações
Rua Dr. Xavier Sigaud, 150 – 4º andar
22290-180 – Rio de Janeiro, RJ
Brazil
E-mail: socorro@cbpf.br/valeria@cbpf.br
http://www.biblioteca.cbpf.br/index_2.html